

AD-A280 207
■■■■■■■■■■

①

InTlSb REPORT

InTlSb for Long-Wavelength Infrared Photodetectors and Arrays

Contract No. N00014-92-J-1951

Manijeh Razeghi

DTIC
ELECTE
JUN 09 1994
S G D

Center for Quantum Devices
Dept. of Electrical Engineering and Computer Science
Northwestern University
Evanston, Illinois 60208

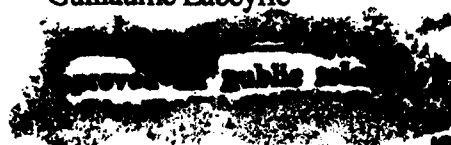
DTIC QUALITY INSPECTED 2

MOCVD material growth and characterization:

Yeun Choi,

Jedon Kim,

Guillaume Labeyrie



94 6 7

0411

148
■■■■■■■■■■
94-17310

INTRODUCTION

The objective of this research program is to grow InTlSb alloys for long-wavelength infrared detectors by low-pressure metalorganic chemical vapor deposition and to investigate their physical properties. As the start towards this goal, optimum growth conditions for high quality InSb epitaxial films on InSb, GaAs, and Si have been determined. InSb films grown under these conditions exhibited one of the best structural and electrical properties reported so far¹⁻³. Growth of InTlSb was then carried out using cyclopentadienylthallium as the source for thallium. This has led to the first successful growth of InTlSb having an extended infrared response⁴⁻⁷. By changing the thallium flow, thallium content was varied and the resulting absorption edge varied from 5.5 μm to 9.0 μm ⁸. For conditions yielding a 9.0 μm absorption edge, a thick sample was grown which resulted in a photoconductor having a specific detectivity of $D^* = 10^9 \text{ cmHz}^{1/2}\text{W}^{-1}$ at 77K and 7 μm . These results demonstrate InTlSb as feasible material system for infrared detection.

Efforts of our research have then been devoted to aspects of material growth related to photovoltaic detector and focal plane array fabrication. Reproducible epitaxial doping, the foremost requirement to realizing photovoltaic detectors, have been first investigate in InSb. Successful n- and p-doping were obtained using Sn and Zn as the respective dopants, without any observable degradation. N- and p-doping of InTlSb were also achieved for the first time to a concentration of $2.5 \times 10^{16} \text{ cm}^{-3}$ and $3 \times 10^{18} \text{ cm}^{-3}$, respectively. In addition, InSb epilayer quality on Si and uniformity of our growths have been improved due to their importance for focal plane array applications. A 6.3 μm -thick InSb epilayer exhibited a X-ray full width half maximum value of 125 arcsec on Si and good uniformity up to an area of 25mm x 40mm was obtained in our MOCVD growths. These are encouraging achievements towards demonstrating InTlSb photovoltaic detectors for focal plane arrays.

1. Doping of InSb and InTlSb

In many III-V semiconductors Si is a widely used n-type dopant. It has been previously demonstrated as a viable n-type dopant for InSb grown by MBE⁹. In our InSb doping investigation by MOCVD, silane (SiH_4) was tentatively used as a Si source of Si. The doping concentration, determined by Hall effect measurements at 77K, indicated no

Availability Codes	
Dist	Avail and/or Special
A-1	

significant doping using silane. This was attributed to low pyrolysis efficiency of silane at our growth temperature of 465°C ¹⁰. In order to determine the validity of this assertion, di-silane (Si_2H_6) which pyrolyze completely at this temperature¹⁰ was used. The di-silane flow rate was varied from 50 to 1500 cc/min. Over this entire range, there was again no conclusive evidence of a doping trend. Furthermore, at flow rates greater than 500 cc/min surface degradation and reduced growth rates were observed; the growth rate reduced from $0.7\mu\text{m/hr}$ to $0.42\mu\text{m/hr}$ when di-silane was introduced at a flow rate of 1500 cc/min. These results could be due to a reaction between the dopant and the metalorganics in the vapor phase or effects arising from impurities in the source.

Following the work of Biefeld et al.¹¹, tetraethyltin (TESn) was purchased from Morton International as an alternative n-type dopant source. The TESn bubbler was kept at a temperature of -25°C and the flow rate was varied from 7cc/min to 80cc/min, resulting in doping levels ranging from $5 \times 10^{16}\text{cm}^{-3}$ to $1.2 \times 10^{18}\text{cm}^{-3}$ (figure 1). No degradation in surface morphology and x-ray FWHM were observed. Furthermore, we did not notice any memory effect associated with TESn, consistent with the reported work¹¹. In order to assess the activation energy of Sn dopant in InSb, the carrier concentration (log scale) as a function of temperature is plotted in figure 2. The kink at higher temperatures (i.e. lower $1/T$) is attributed to the intrinsic valence to conduction band thermal excitation, which can dominate the transport property in low-doped InSb at temperatures above $\sim 200\text{K}$ ². Since

$$\text{ionized carrier concentration} \propto \exp(-E_i/kT)$$

where E_i is the activation energy, k is the Boltzmann's constant and T the temperature, E_i can be assessed from the slope ($-E_i/k$) of the plot. From figure 2, E_i is roughly estimated to be a few tenth of meV.

P-doping of InSb was carried out using dimethylzinc (DMZn). Its bubbler was maintained at a constant temperature at -25°C . The zinc flow was diluted after passing through the bubbler. The dilution flow was kept at 1200 cc/min. Using a 100cc/min capacity mass flow controller, only concentrations greater than $8 \times 10^{18}\text{cm}^{-3}$ were obtained. In order to have a better low flow rate control, a smaller capacity mass flow controller (10cc/min) was installed. This enabled us to lower the doping concentration to approximately $3 \times 10^{18}\text{cm}^{-3}$ (figure 3). To further extend our p-doping ranges to lower levels, diethylzinc (DEZn) has recently been purchased to replace DMZn. DEZn has a much lower vapor pressure than DMZn and is the preferred zinc source for p-type doping of III-V epitaxial alloys. Figure 4 shows the carrier dependence on inverse temperature of a p-type InSb sample. From the

slope, the activation energy of Zn in InSb is estimated to be a few meV. The kink observed in figure 2 is not observed because of the high p-doping level ($\sim 3 \times 10^{18} \text{ cm}^{-3}$), which is approximately 2 orders greater than the intrinsic carrier concentration in this temperature range¹².

Once the doping of InSb has been realized, doping of InTlSb epitaxial films has been attempted using the same dopant sources. InTlSb was n-doped to a level of $2.5 \times 10^{16} \text{ cm}^{-3}$ at a TESn flow rate of 7.5cc/min. P-doping concentration of $3 \times 10^{18} \text{ cm}^{-3}$ was achieved at a minimum DMZn flow rate of 0.1 cc/min. Comparing these data to those in figures 1 and 3, indicates similar doping characteristics for InSb and InTlSb using Sn and Zn.

2. InSb on GaAs-coated Si substrate

Epitaxial film growth of InSb and its alloys on silicon substrate is an attractive subject because of the possibility for integrating infrared detector arrays and signal processing circuits on the same substrate. This can eliminate problems associated with complicated etch-thinning process and indium bump contacts in the hybrid case. The greatest difficulty associated with the growth of high-quality InSb on Si is the very large lattice mismatch (19%) between the two materials. Employing a GaAs buffer layer can greatly improve the quality of InSb layer because of the reduced mismatch from 19% to 15%. In this view, we have previously grown a high-quality InSb film on GaAs-coated Si substrate that exhibited one of the best structural qualities for comparable InSb film thickness on Si¹. To be able to grow InSb alloys such as InTlSb on Si in the future, we have continued to improve InSb epilayer quality on Si.

The growths were carried out on GaAs-coated Si substrates from Kopin corporation. Compared to our previous growth¹, the temperature was lowered by approximately 10°C. As a result, the optimum V/III ratio increased from the previous value of 8.5 to 14 while the growth rate decreased from 1.5 $\mu\text{m/hr}$ to 0.7 $\mu\text{m/hr}$. Several InSb films of various thicknesses were grown under this new condition. The surface morphology of the samples were then observed using Nomarski interference microscope and the structural quality was evaluated from X-ray diffraction measurements. The epilayers were mirror-like. X-ray FWHM values indicate improving crystal quality with increasing epilayer thickness, most likely due to reduced dislocation density away from the InSb-GaAs interface. Figure 5 shows this trend. A 6.3 μm -thick InSb epilayer exhibited a FWHM of 125 arcsec, which is comparable to the values obtained for growths on GaAs substrates.

3. Growth Uniformity

Uniformity of our MOCVD growth has also been addressed due to its importance for focal plane array applications. Two different growth aspects have been considered to improve the uniformity: precursors and temperature gradient. As reported elsewhere, trimethylindium (TMI) and trimethylantimony (TMSb) have been used as our precursors for In and Sb, respectively. Although methyl alkyls are commercially available in high purity grades, they are also stable compounds at low temperatures because of their strong hydrocarbon bond strengths¹⁰. This can be a problem in growing InSb and its alloys when the growth temperatures are kept well below 500°C since the melting point of InSb is 525°C. In our InSb and InTlSb growth temperature range of 430-465°C range, incomplete decomposition of the precursors have been reported¹³. This can lead to non-uniform growths in the presence of some temperature gradient because of different decomposition rates.

Triethylindium (TEI), whose hydrocarbon bond strengths are weaker than those of TMI, was the first alternative precursor available. Its decomposition temperature can be as low as 40°C¹⁵ and hence was expected to enhance our growth uniformity. The TEI bubbler temperature was maintained at 30°C so that reasonable vapor pressure can be obtained. The growth temperature and TMSb flow rate was kept at the optimum values determined previously for InSb growth¹. Growth of InSb was then attempted at various TEI flow rates but was unsuccessful. The investigated V/III ratio covered a wide range from 10 to 230. At V/III ratios higher than 57, we observed no film deposition for a growth duration of 20 minutes. At lower V/III ratios (higher In flow rates), In droplets formed on the surface but still without any film deposition. There were also some deposition observed at the inlets of the growth chamber. These observations were attributed to instability of TEI, especially in the presence of hydrogen¹⁴, which is being used as our carrier gas. Therefore, In source was switched back to TMI since then. There are few alternative Sb sources such as triethylantimony¹⁵ and triisopropylantimony^{16,17} that are also expected to improved the growth uniformity. However, these sources are not currently available in our laboratory and are being considered for future studies.

As the next step to improve the uniformity, investigation on the temperature gradient along our MOCVD susceptor was carried out. Temperature mapping of the susceptor revealed a difference as large as 10-12°C. In order to reduce this, the rf-coil of the MOCVD was

reconfigured. This involved adjustment of the coil spacing, so that areas of lower temperature are exposed to higher electromagnetic flux density than the higher temperature regions. The adjustment has resulted in a temperature difference of less than 5°C between the bottom and top of our susceptor. This improvement was reflected upon our subsequent InSb growth experiments on large areas (25mm x 40mm) where the difference in the film thicknesses over the entire area were within the experimental error of the thickness measurements.

CONCLUSION

Reproducible growth of high quality InSb films have been mastered and the first successful growth of InTlSb was demonstrated. Study of the InTlSb alloy bandgap tailoring, by means of varying its composition, was then performed. This work resulted in the growth of various alloys, with maximum photoresponse cutoff wavelength up to $9.5\mu\text{m}$. It also lead to the fabrication of a photoconductor with a specific detectivity of $D^*=10^9 \text{ cmHz}^{1/2}\text{W}^{-1}$ at $\lambda=7\mu\text{m}$ and 77K.

Once this phase of this program was achieved, investigations aimed at realizing photovoltaic detectors and focal plane arrays were carried out. Doping of InSb has been investigated as the initial step. After considering various n-type dopants, reproducible n-doping have been obtained using tetraethyltin in the concentration range from $5 \times 10^{16} \text{ cm}^{-3}$ to $1.2 \times 10^{18} \text{ cm}^{-3}$. P-type doping of InSb was achieved using dimethylzinc in the range of $3.0 \times 10^{18} \text{ cm}^{-3}$ to $3 \times 10^{19} \text{ cm}^{-3}$. With the same dopant sources, N- and p-doping of InTlSb were also realized for the first time. As the next step, uniformity of the MOCVD growths and InSb epilayer quality on Si substrate have been improved. A $6.3 \mu\text{m}$ -thick InSb epilayer on GaAs-coated Si showed mirror-like morphology and x-ray FWHM of 125 arcsec.

FUTURE WORK

Measurements from our initial InSb photovoltaic detectors, indicate a need to lower the doping levels to decrease the dark current originating from tunneling. Therefore, efforts will be given to this aspect in order to optimize photovoltaic detector performance. More doping investigation on InTlSb will be also carried out to better understand the doping behaviour and limit in InTlSb. Once this is complete, photovoltaic detector based on InTlSb will be fabricated and demonstrated.

Investigations on improving the X-ray full-width-at-half-maximum of InTlSb epilayers and increasing the thallium content are being continued. The results so far do not indicate any fundamental limitation to these improvements. Therefore, the investigation in this research area will be actively pursued.

We plan to further investigate the optical properties of InTlSb using infrared photoluminescence. For this purpose, the necessary equipments were ordered to upgrade an existing luminescence set-up operating in the visible to near-infrared. These parts have arrived and will be set-up in the near future. This will allow us to study the luminescence properties of the epilayers, compare the optical properties of the epilayers grown on InSb and GaAs substrate, and assess the epitaxial layer uniformity.

REFERENCES

1. Y.H. Choi, R. Sudharsanan, C. Besikci, E. Bigan, and M. Razeghi, Mat. Res. Soc. Symp. Proc. 281, 375, 1993.
2. C. Besikci, Y.H. Choi, R. Sudharsanan, and M. Razeghi, J. Appl. Phys. 73, 5009, 1993.
3. S.N. Song, J.B. Ketterson, Y.H. Choi, R. Sudharsanan, and M. Razeghi, Appl. Phys. Lett. 63, 964, 1993.
4. Y.H. Choi, C. Besikci, R. Sudharsanan, and M. Razeghi, Appl. Phys. Lett. 63, 361, 1993.
5. M. Razeghi, Y.H. Choi, P.T. Staveteig, and E. Bigan, Proceedings of the 184th meeting of the Electrochemical Society, New Orleans, Louisiana, October, 1993.
6. Y.H. Choi, P.T. Staveteig, E. Bigan, and M. Razeghi, J. Appl. Phys. 75, 3196, 1994.
7. P.T. Staveteig, Y.H. Choi, G. Labeyrie, E. Bigan, and M. Razeghi, Appl. Phys. Lett. 64, 460, 1994.
8. E. Bigan, Y.H. Choi, G. Labeyrie, E. Bigan, and M. Razeghi, Proceedings of SPIE, Los Angeles, California, January 1994.
9. R.A. Stradling, Semicond. Sci. Technol. 6, C52, 1991.
10. G.B. Stringfellow, *Organometallic Vapor-Phase Epitaxy: Theory and Practice*, (Academic, New York), 1989.
11. R.M. Biefeld, J.R. Wendt, and S.R. Kurtz, J. of Crystal Growth 107, 836, 1991.
12. Y.J. Jung, M.K. Park, S.I. Tae, K.H. Lee, and H.J. Lee, J. Appl. Phys. 69, 3109, 1991.
13. C.H. Chen, Z.M. Fang, G.B. Stringfellow, and R.W. Gedridge, Jr., J. Appl. Phys. 69, 7605, 1991.
14. CVD Metalorganics for Vapor Phase Epitaxy, Product Guide and Literature Review II, Morton International, Advance Materials
15. R.M. Biefeld and G.A. Hebner, Appl. Phys. Lett. 57, 1563, 1990.
16. G.T. Stauf, D.K. Gaskill, N. Bottka, and R.W. Gedridge, Jr., Appl. Phys. Lett. 58, 1311, 1991.
17. C.H. Chen, Z.M. Fang, G.B. Stringfellow, and R.W. Gedridge, Jr., Appl. Phys. Lett. 58, 2532, 1991.

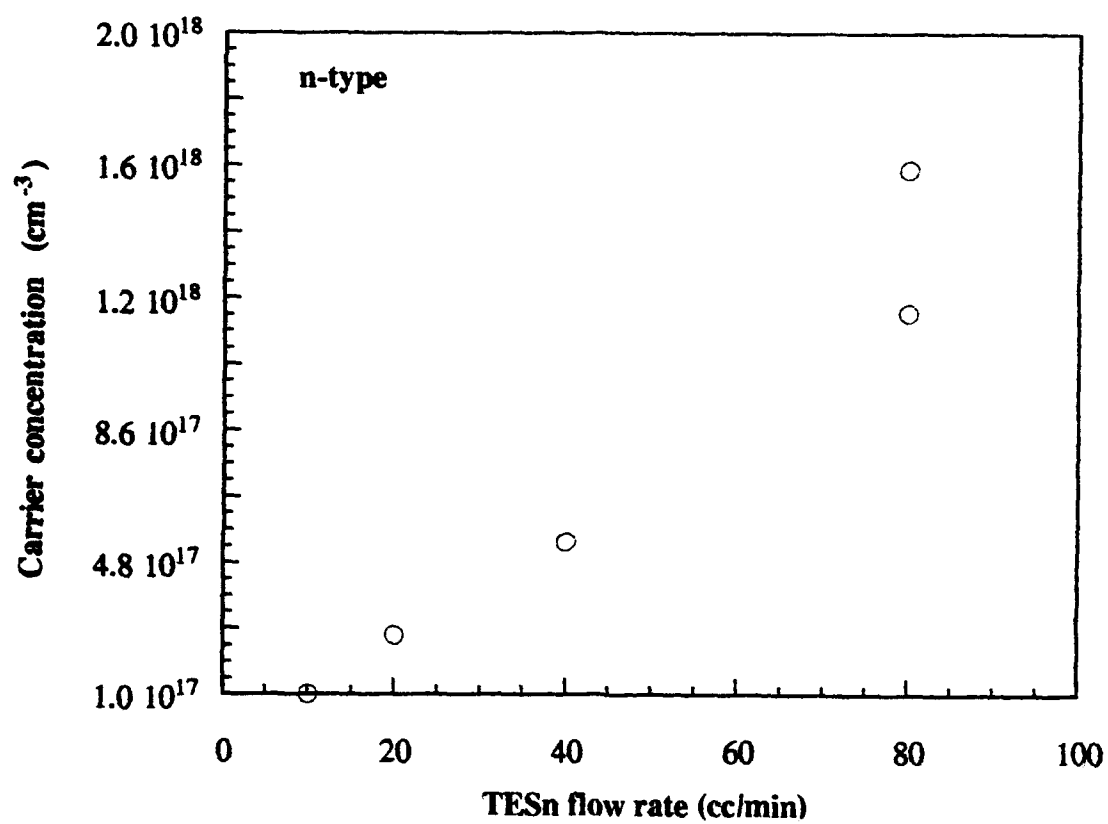


FIGURE 1 - N-doping concentration dependence on TESn flow rate

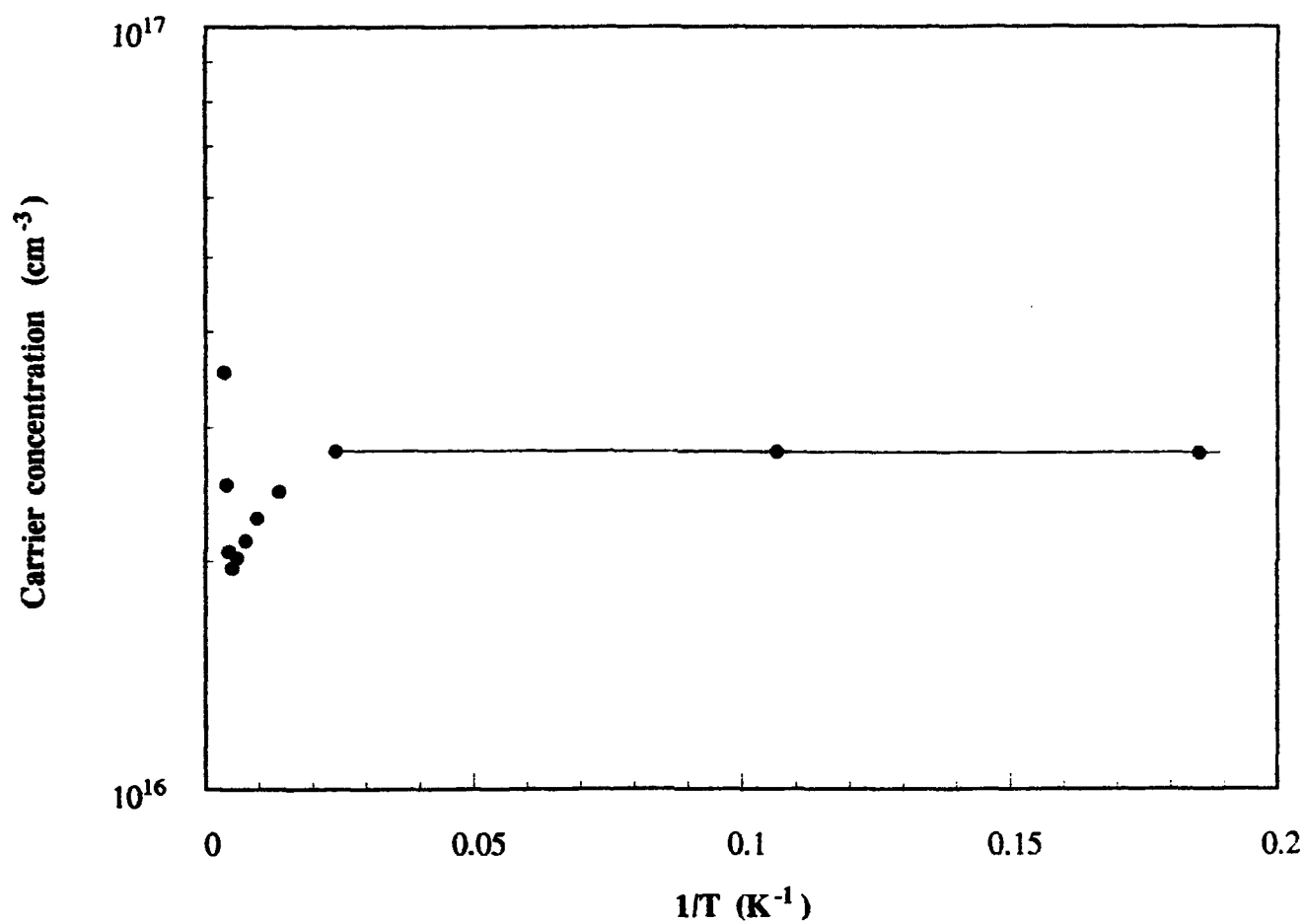


FIGURE 2 - Plot of net donor concentration versus inverse temperature

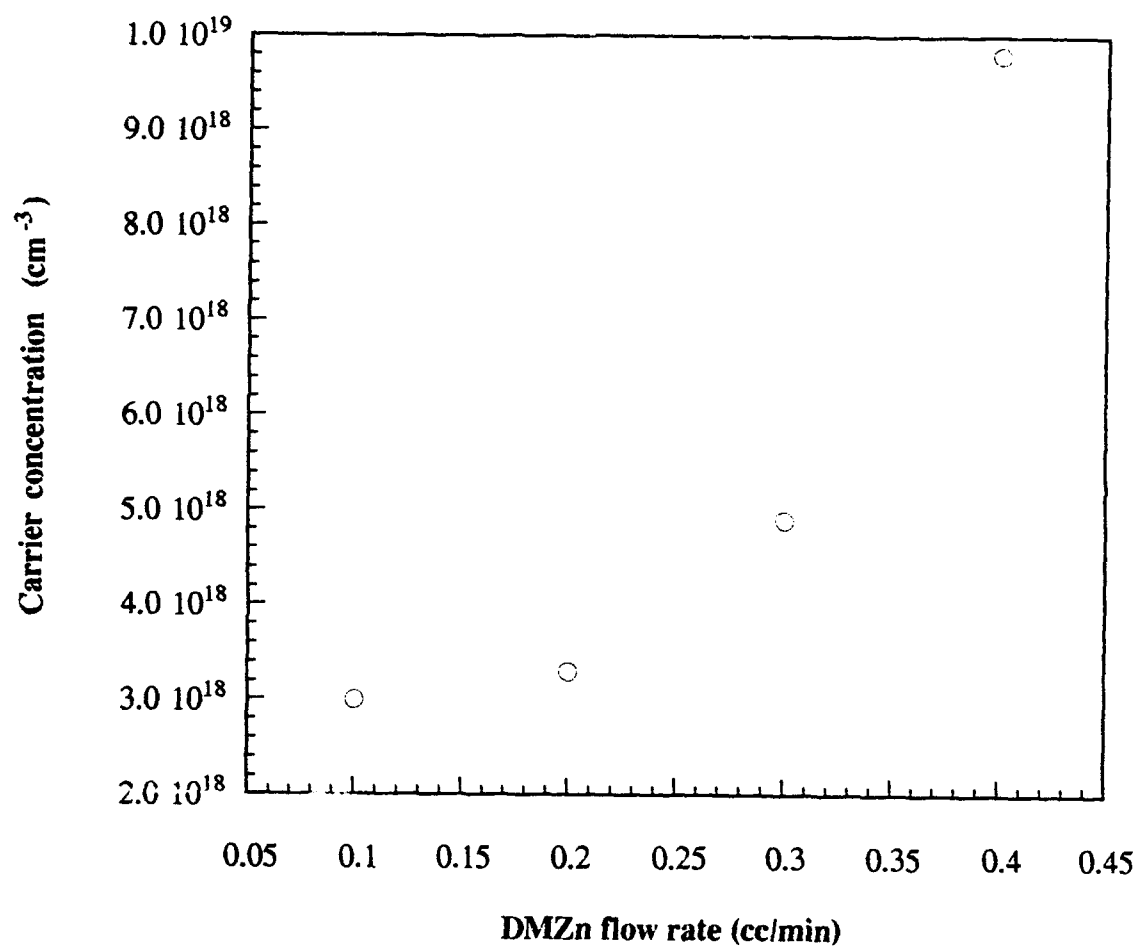


FIGURE 3 - P-doping concentration as a function of DMZn flow rate

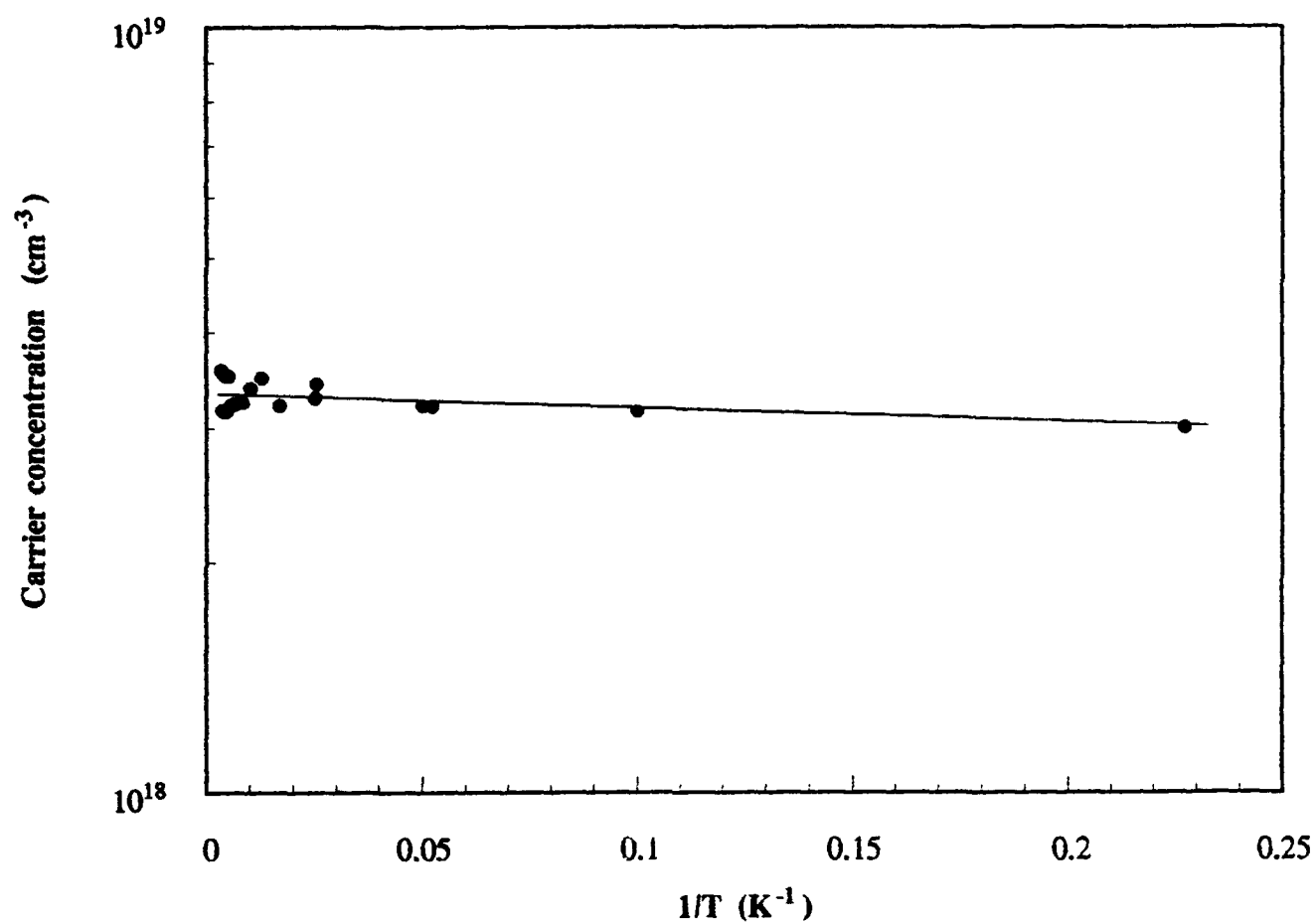


FIGURE 4 - Plot of hole concentration versus inverse temperature

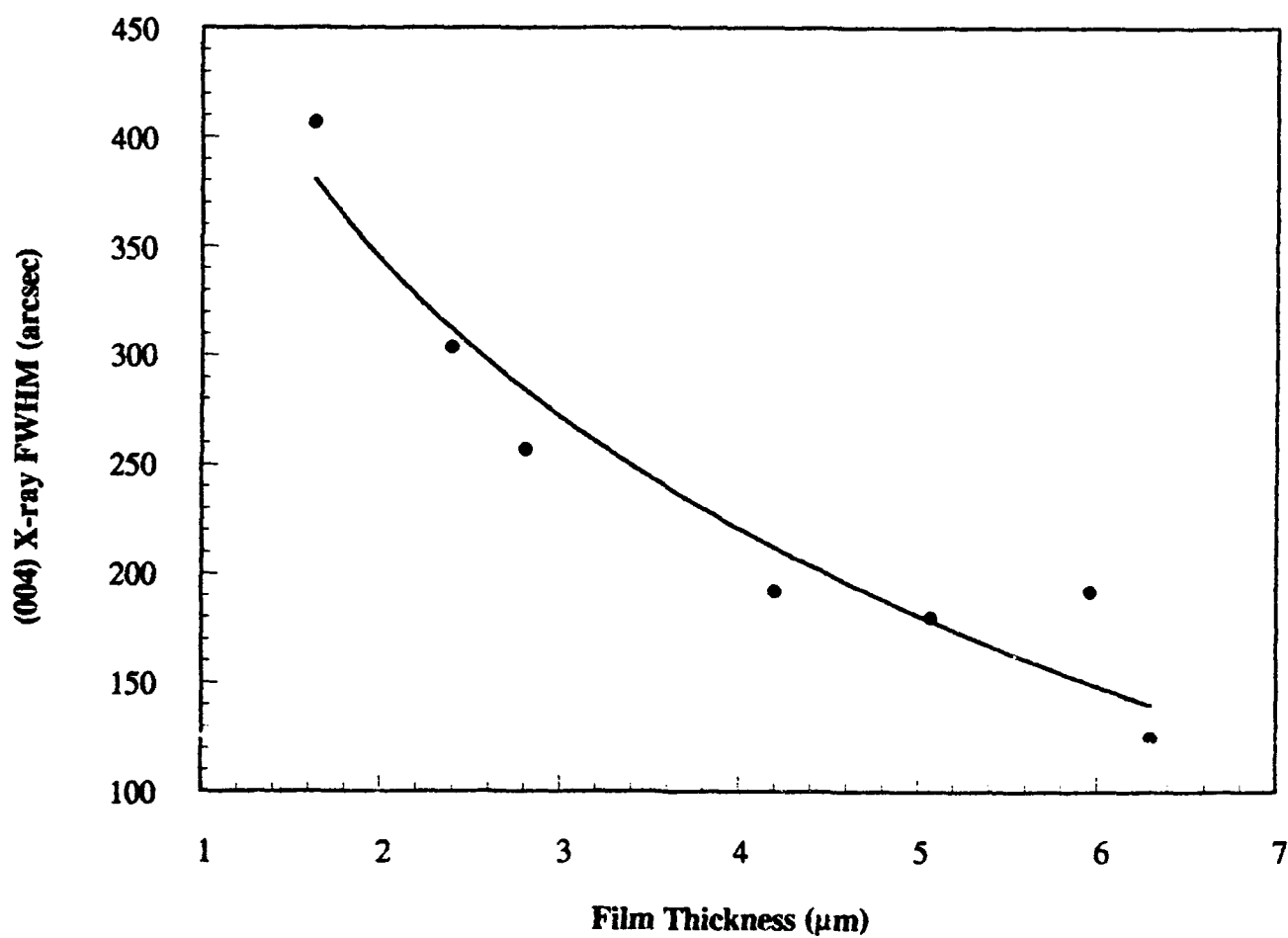


FIGURE 5 - X-ray FWHM dependence on thickness of InSb on GaAs-coated Si